Supplemental Information

Profiling of the Immune Landscape in Murine Glioblastoma following Blood Brain/Tumor Barrier Disruption with MR Image-guided Focused Ultrasound

Natasha D. Sheybani[1], Alexandra R. Witter[2], William J. Garrison[1], G. Wilson Miller[3], Richard J. Price[1,3], Timothy N.J. Bullock[2]

1. Department of Biomedical Engineering, University of Virginia, Charlottesville, VA
2. Department of Pathology, University of Virginia, Charlottesville, VA
3. Department of Radiology and Medical Imaging, University of Virginia, Charlottesville, VA

Corresponding Authors:
Timothy N.J. Bullock, Ph.D.
Email: tb5v@virginia.edu

Richard J. Price, Ph.D.
Email: rprice@virginia.edu

Natasha D. Sheybani, Ph.D.
Email: nds3sa@virginia.edu

Supplemental Figures

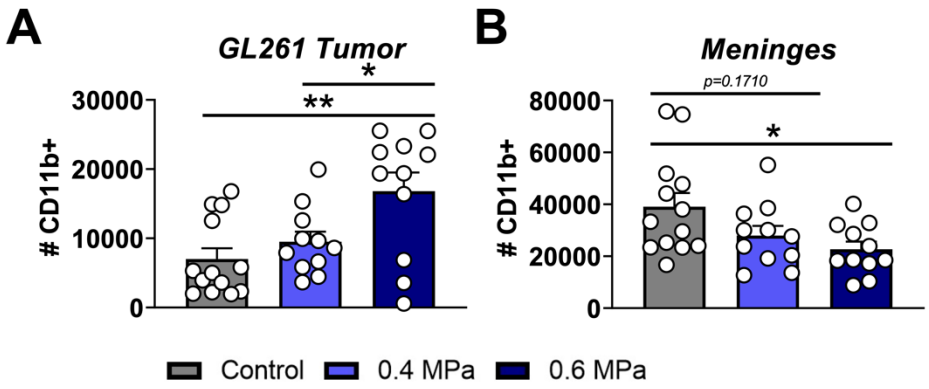

Figure S1. Myeloid cell representation in GL261 tumors and meninges at Day 21 post-implantation. (A-B) Absolute number of CD11b+ myeloid cells in tumor (A) and meninges (B). n=11-13 per group. Data reported for 2 independent experiments.

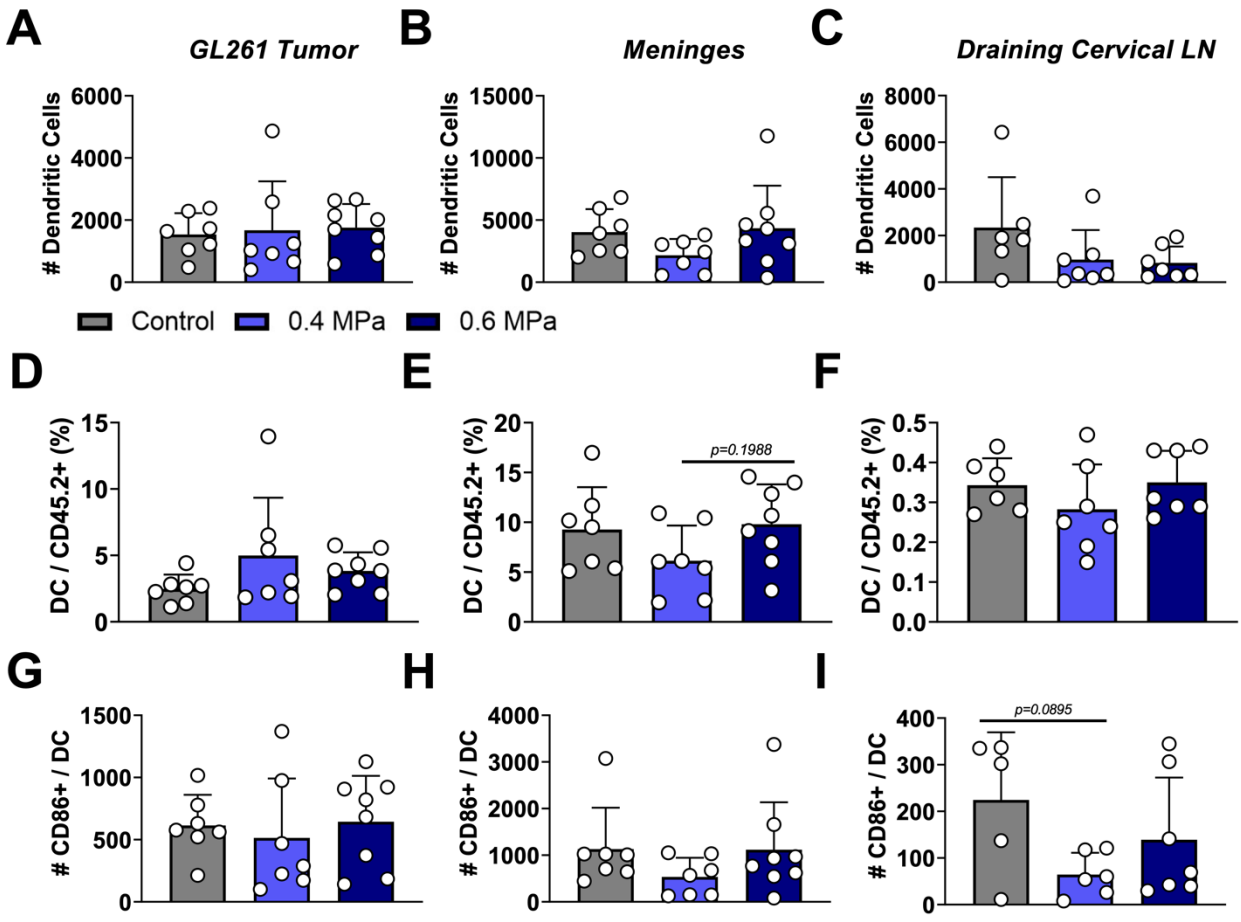

Figure S2. Dendritic cell representation in tumors, meninges and draining cervical lymph nodes at Day 28 post-implantation. (A-C) Absolute number of CD11c-hi in GL261 tumors (A), meninges (B) and draining cervical lymph nodes (C). (D-F) Percentage of CD11c-hi dendritic cells out of CD45.2+ immune cells in GL261 tumors (D), meninges (E) and draining cervical lymph nodes (F). (G-I) Absolute number of CD86+ CD11c-hi dendritic cells in GL261 tumors (G), meninges (H) and draining cervical lymph nodes (I). n=5-8 per group. Data reported for 1 representative experiment.

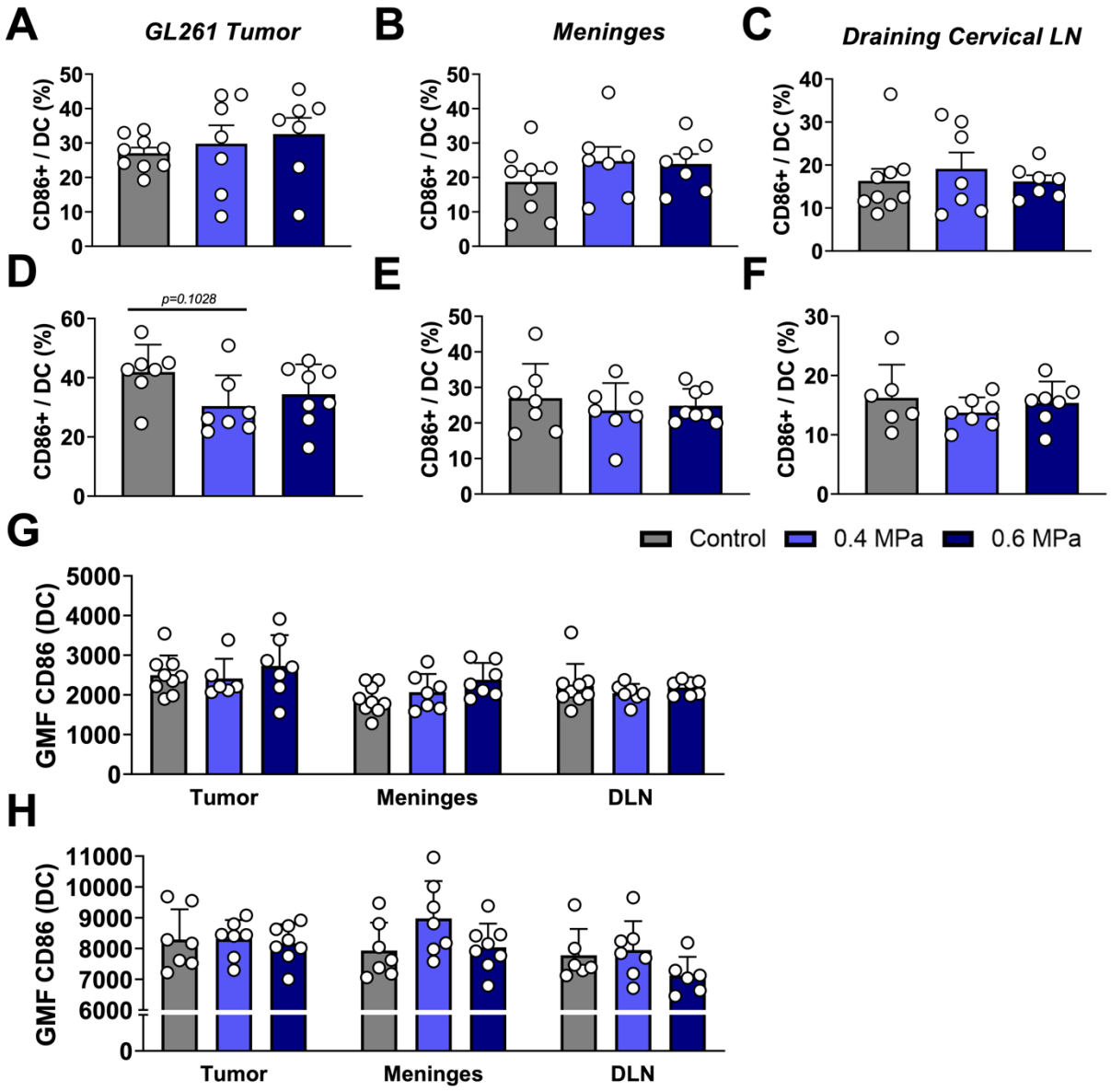

Figure S3. CD86 expression on dendritic cells in tumors, meninges and draining cervical lymph nodes of control or FUS-treated GL261-bearing mice. (A-F) Percentage of CD11c-hi dendritic cells expressing CD86 in tumor (A,D), meninges (B,E), and draining cervical lymph nodes (C,F) at Days 21 (A-C) and 28 (D-F) post-implantation. (G-H) Geometric fluorescence intensity (GMF) of CD86 on dendritic cells across tissues at Days 21 (G) and 28 (H) post-

implantation. Data reported for one representative experiment. n=6-9 per group. Data reported for 1 representative experiment.

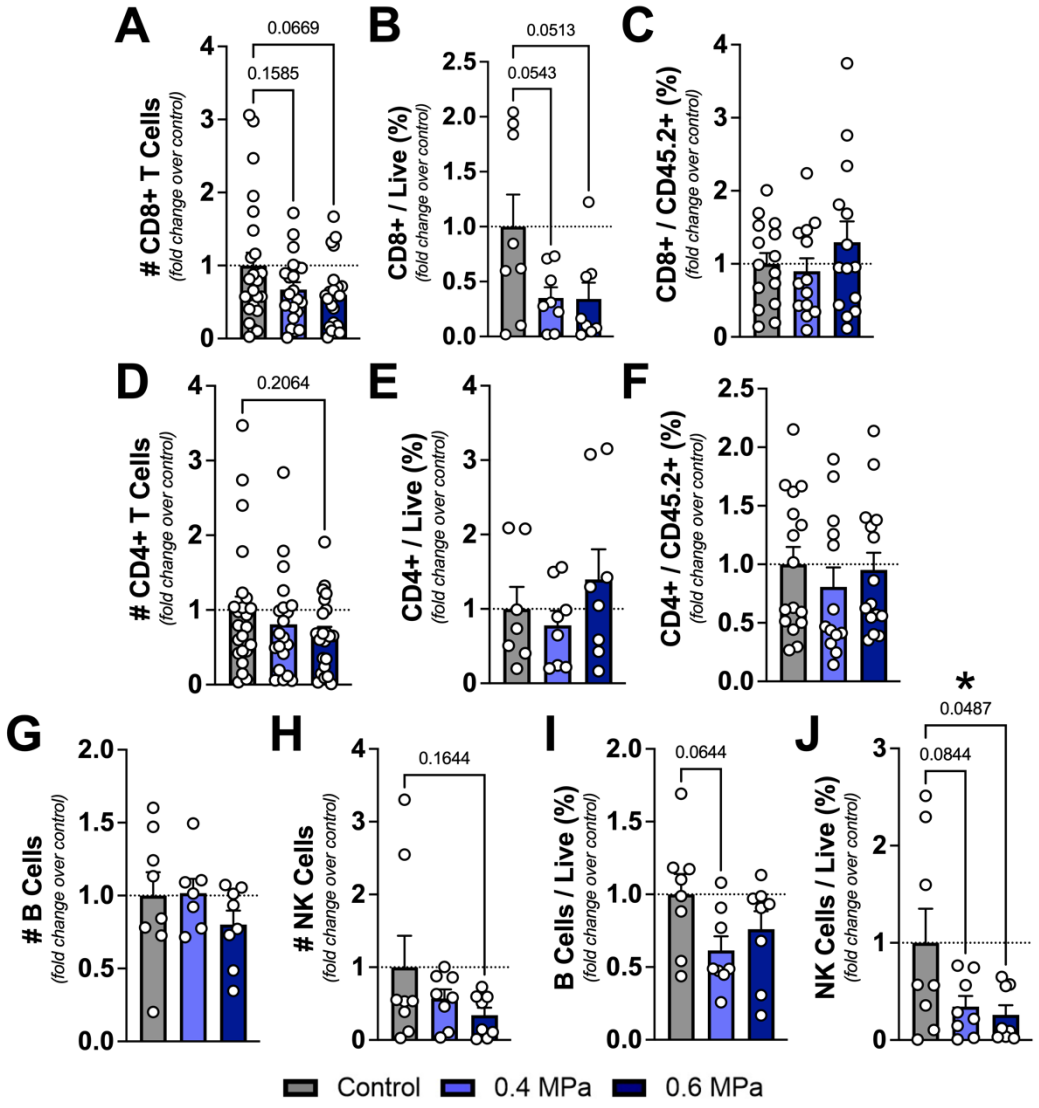

Figure S4. Adaptive immune cell representation in meninges of GL261-bearing mice at Day 21 post-implantation. (A) Fold change in absolute number of CD8+ T cells in meninges. (B-C) Fold change in percentage of CD8+ T cells out of live cells (B) or CD45.2+ immune cells (C) in meninges. (D) Fold change in absolute number of CD4+ T cells in meninges. (E-F) Fold change in percentage of CD4+ T cells out of live cells (E) or CD45.2+ immune cells (F) in meninges. (G-H) Fold change in absolute number of B (G) and NK (H) cells in meninges. (I-J) Fold change in percentage of B (I) or NK (J) cells out of live cells in meninges. n=7-24 per group. Data reported for 2-4 independent experiments.

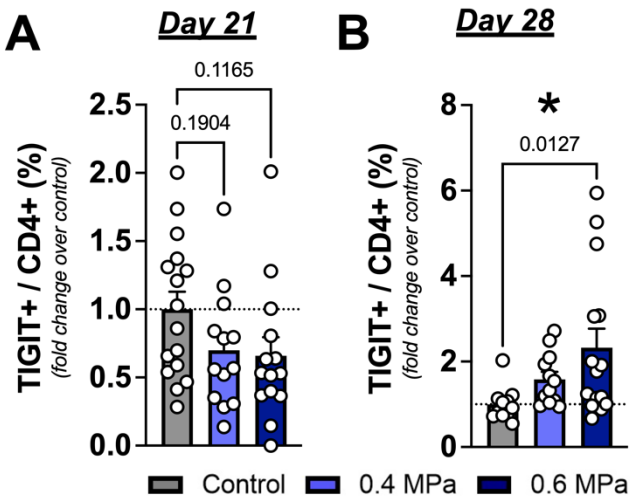

Figure S5. TIGIT expression in draining cervical lymph nodes. (A-B) Fold change in percentage of TIGIT-expressing CD4+ T cells at Day 21 (A) and Day 28 (B) post-implantation. n=11-16 per group. Data reported for 2 independent experiments.

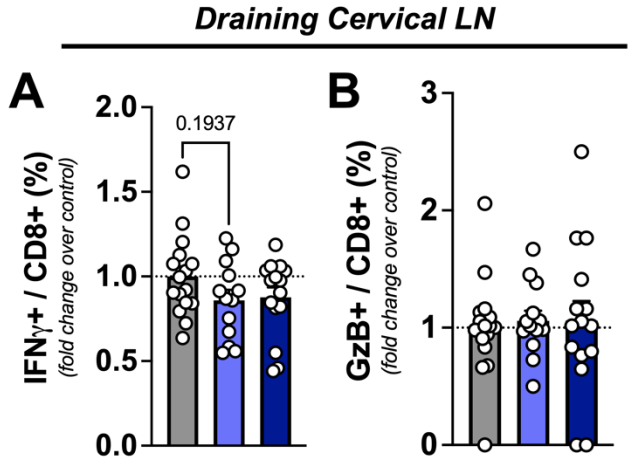

Figure S6. Functional assessment of CD8+ T cells in draining lymph nodes. (A-B) Fold change in percentage of CD8+ T cells expressing interferon-γ (IFN-γ) (A) or granzyme-B (GzB) (B) in draining lymph nodes at Day 21 post-implantation. n=12-16 per group. Data reported for 2 independent experiments.

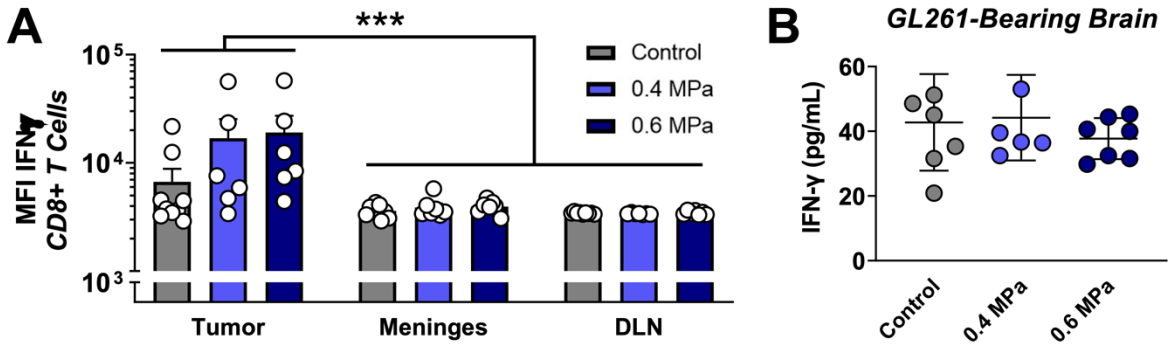

Figure S7. IFN-γ expression by CD8+ T cells from control or FUS-treated GL261-bearing mice. (A) Representative MFI of IFN-γ on CD8+ T cells across tissues at Day 21. (B) Global IFN-γ concentration within supernatants isolated from whole GL261-bearing brain homogenates as determined by ELISA. n=5-9 per group. Data reported for 1 representative experiment.

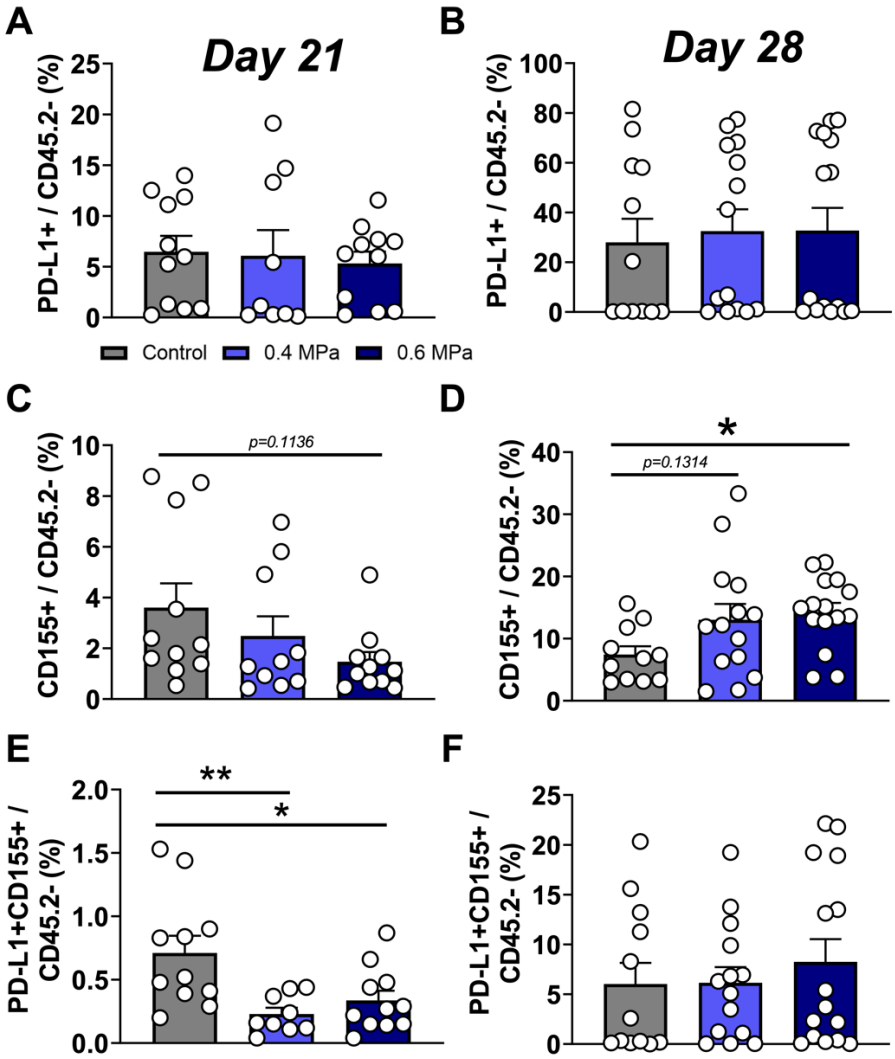

Figure S8. Checkpoint ligand expression on non-immune cells in GL261 tumors. (A-B) Percentage of non-immune CD45.2- (tumor/stromal) cells expressing PD-L1 in GL261 tumors at Days 21 (A) and 28 (B) post-implantation. (C-D) Percentage of CD45.2- cells expressing CD155 in GL261 tumors at Days 21 (C) and 28 (D) post-implantation. (E-F) Percentage of CD45.2- cells dually expressing PD-L1 and CD155 in GL261 tumors at Days 21 (E) and 28 (F) post-implantation. n=9-15 per group. Data reported for 2 independent experiments.

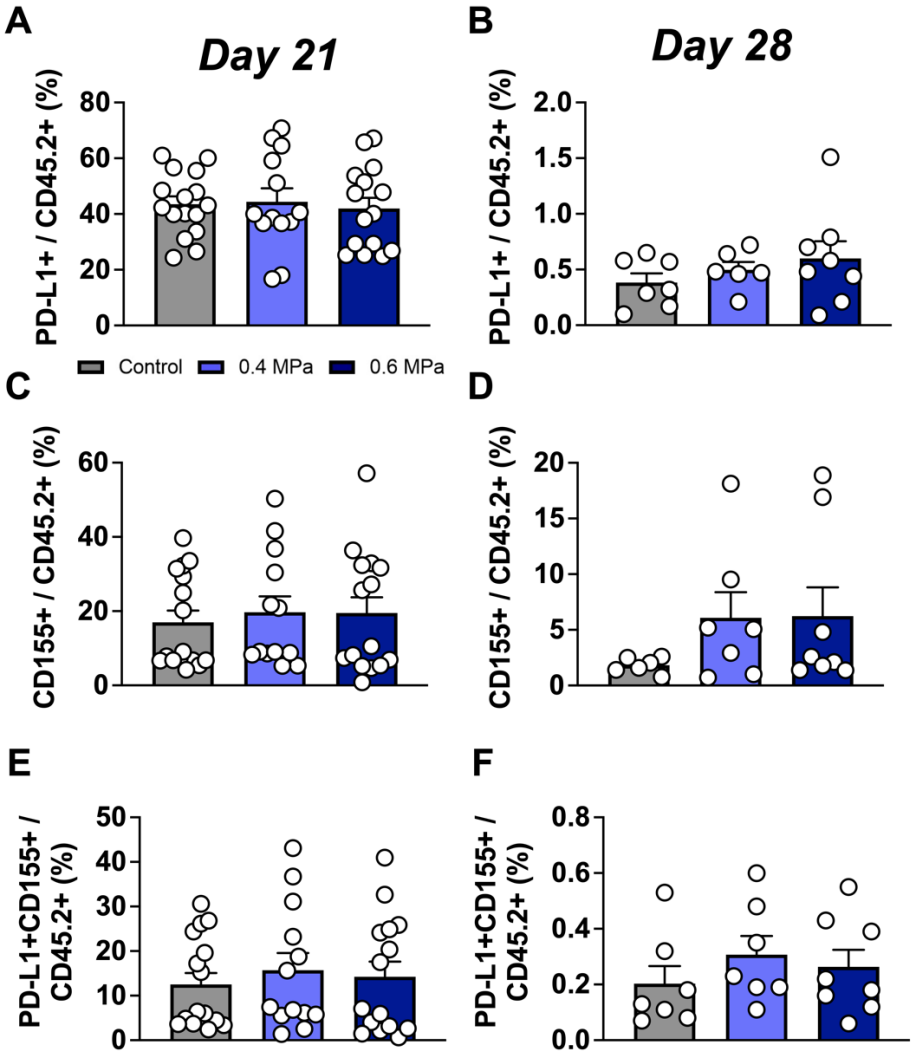

Figure S9. Checkpoint ligand expression on immune cells in GL261 tumors. (A-B) Percentage of immune CD45.2+ cells expressing PD-L1 in GL261 tumors at Days 21 (A) and 28 (B) post-implantation. (C-D) Percentage of CD45.2+ cells expressing CD155 in GL261 tumors at Days 21 (C) and 28 (D) post-implantation. (E-F) Percentage of CD45.2+ cells dually expressing PD-L1 and CD155 in GL261 tumors at Days 21 (E) and 28 (F) post-implantation. n=6-16 per group. Data reported for 1-2 independent experiments.

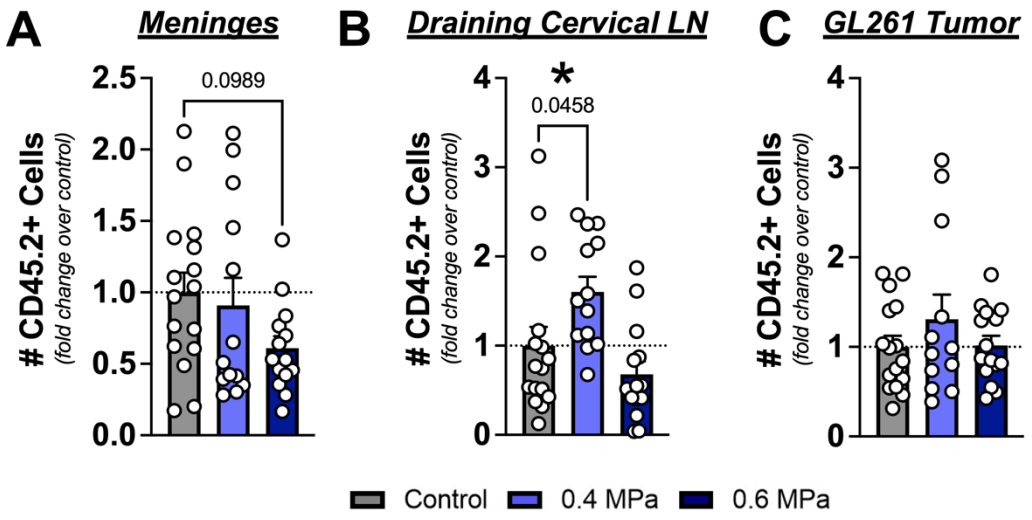

Figure S10. Overall immune cell representation across organs. (A-B) Fold change in absolute number of CD45.2+ immune cells in GL261 tumors (A), draining cervical lymph nodes (B) and meninges (C) at Day 21 post-implantation. n=12-16 per group. Data reported for 2 independent experiments.

Supplemental Methods

Passive Cavitation Detection

Acoustic emissions were detected with a 2.5 mm wideband unfocused hydrophone mounted in the center of the transducer. Acoustic signal was captured using a scope card (ATS460, Alazar, Pointe-Claire, Canada) and processed using an in-house MATLAB algorithm. Acoustic emissions at the fundamental frequency, harmonics (2f, 3f, 4f), sub harmonic (0.5f), and ultra-harmonics (1.5f, 2.5f, 3.5f) were assessed by first taking the root mean square of the peak spectral amplitude (Vrms) in each frequency band after applying a 5 kHz bandwidth filter, and then summing the product of Vrms and individual sonication duration over the entire treatment period. Inertial cavitation was assessed by summing the product of Vrms and individual sonication duration for all remaining emissions (broadband) over the entire treatment period.

MR Imaging

Contrast-enhanced MR imaging used a T1-weighted spoiled gradient-echo 3D pulse sequence. 3T MRI parameters included: TR/TE = 12/4.35 ms, readout bandwidth = 300 Hz/pixel, flip angle = 20◦, matrix = 128 × 256 × 120, voxel size = (0.3 mm)3 , acquisition time = 3:04.

Flow Cytometry

Tumor-bearing brains were mechanically disaggregated then centrifuged at 290 rcf for 5 mins. Following this spin step, supernatants were removed and stored at -20°C. Spleen, DCLN, SLN, and meninges were mechanically homogenized and filtered through 100 µm Nitex nylon mesh. Spleen, meninges, and blood samples were RBC lysed (Hybri-Max; Sigma #R7757). Brain homogenates were incubated with 100 µL DNase I (30 mg/mL stock; grade II, from bovine pancreas; Sigma/Roche #10104159001) and 10 uL Collagenase/Dispase (100 mg/mL stock; Sigma/Roche #10269638001) for 45 mins at 37 C on a rotator. Homogenates were washed once with RT 1xPBS and filtered through 70 µm mesh. Brain cells then underwent one of two methods for myelin removal and leukocyte isolation.

(1) Brain cells were resuspended in 20 mL 60% Percoll (60% Buffered Percoll+40% RPMI), then 20 mL 30% Percoll (30% Buffered Percoll+70% 1xPBS) (Sigma #P1644). Samples were carefully layered on top to create two distinct layers. Gradients were centrifuged for 25 mins at 805 rcf with no brake. The myelin layer (top) was discarded while the lymphocyte layer (interface) and pellet of tumor/stromal cells were isolated separately for staining. (2) Brain cells were resuspended in 40% Percoll solution and centrifuged to separate the myelin layer, following which this layer discarded with surrounding supernatant. The remaining cell pellet was resuspended in 1xPBS and subsequently underlayered with Lympholyte M solution. Following centrifugation, the lymphocyte layer and tumor pellet were isolated separately for staining.

Samples were split across two panels and stained in 96 well V-bottom plates. Viability (Live/Dead) staining was performed in 1xPBS, following which all subsequent steps were performed in FACS buffer supplemented with 2% normal mouse serum. To reduce non-specific binding, cells were incubated with Fc block for 15 mins prior to antibody staining. The following antibodies were used for staining of cell surface proteins: T cell panel - CD4 BV650 (BD Biosciences #563232), CD8a PE-Cy7 (ThermoFisher/eBio #25-0081-82), NKp46 PE (ThermoFisher/eBio #12-3351-82), CD44 AF700 (ThermoFisher/eBio #56-0441-82), PD1/CD279 BV605 (BioLegend #135220), TIM3 APC (BioLegend #134008), TIGIT PE-Dazzle594 (BioLegend #142110), CD19 eFluor450 (ThermoFisher/eBio #48-0193-82); Myeloid panel - F4/80 BV421 (BioLegend #123131), CD11b AF700 (BioLegend #101222), CD86 BV650 (BioLegend #105035), CD11c PE (ThermoFisher/eBio #12-0114-82), Ly6C PE-Dazzle594 (BioLegend #128044), Ly6G BV605 (BioLegend #127639). Following surface staining, cells were fixed and permeabilized using the Transcription Factor Staining Buffer Set (Life Technologies #00-5523-00), following which intracellular staining was conducted with the following antibodies: FoxP3 PerCP-Cy5.5 (ThermoFisher/eBio #45-5773-82), Granzyme-B PE-Cy7 (ThermoFisher #25-8898-82) and IFN-gamma APC (ThermoFisher #17-7311-82).